

# Nugget formation and growth during resistance spot welding of aluminium alloy 5182

M. Rashid<sup>1,2</sup>, J. B. Medley<sup>2</sup> and Y. Zhou<sup>2</sup>

Surface interaction at the worksheet/worksheet interface during resistance spot welding of aluminium alloy 5182 with spherical tip electrodes was investigated. Oxide layer cracking and nugget formation were focused. Both experimental work and finite element analysis were employed to explain the contact behaviour at this interface. It was found that sheet separation and thus bending occurred during the squeezing phase of the resistance spot welding process and suggested a profound influence on nugget formation. The sheet separation caused enlarged and aligned cracks in the surface oxide layers which led to a good metal-to-metal contact near the periphery of the faying surface. High current densities which occurred at the beginning of the current phase caused significant heat generation in this zone. Consequently, the melting at the faying surface started near the periphery and moved in towards the central zone of the contact region to produce a 'doughnut shaped' nugget with a filled-in but thin central region.

On a étudié l'interaction de la surface à l'interface feuille de travail-feuille de travail lors du soudage par points par résistance de l'alliage d'aluminium 5182 avec des électrodes à bout sphérique. On s'est concentré sur la fracture de la couche d'oxyde et sur la formation du noyau. On a utilisé tant le travail expérimental que l'analyse par éléments finis pour expliquer le comportement de contact à cette interface. On a trouvé que la séparation de la feuille, et donc le pliage, se produisait lors de la phase de compression du procédé de soudage par points par résistance, suggérant une influence profonde sur la formation du noyau. La séparation de la feuille résultait en fissures agrandies et alignées dans les couches d'oxyde de la surface, ce qui amenait un bon contact de métal à métal près de la périphérie de l'aire de contact. Des densités élevées de courant, qui se produisaient au début de la phase de courant, résultaient en un dégagement important de chaleur dans cette zone. Conséquemment, la fonte de l'aire de contact commençait près de la périphérie et se déplaçait vers la zone centrale de la région de contact, produisant un noyau en forme d'anneau avec une région centrale remplie, mais mince.

**Keywords:** Resistance spot welding, Aluminium alloy, Faying surface, Sheet separation, Oxide layer, Nugget formation

## Introduction

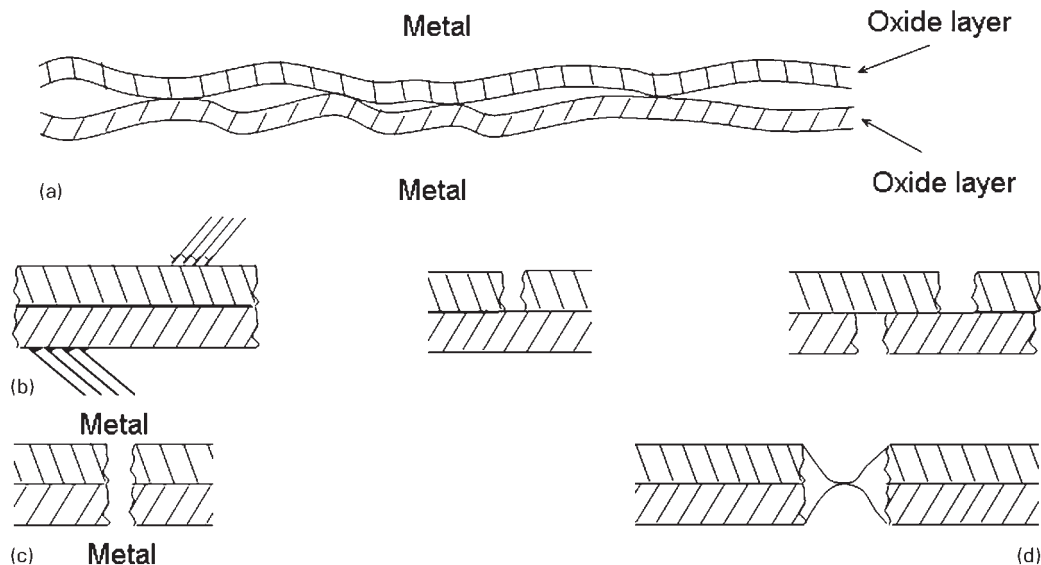
Resistance spot welding (RSW) has been one of the most popular joining processes for sheet metal applications particularly for auto body frames and panels.<sup>1,2</sup>

However, understanding the process for a particular material is essential for successful application. Although, the basic principle is the same, RSW of aluminium alloys differs significantly than that of steel. The main source of heating during RSW of aluminium alloys comes from the electrical contact resistance at the interfaces,<sup>3-5</sup> which makes it an important variable for this material. This electrical contact resistance at worksheet/worksheet interface or faying surface (FS) provides the necessary heat generation for nugget formation.<sup>6</sup> However, the electrical contact resistance at the electrode/

<sup>1</sup>CANMET-MTL, Natural Resources Canada, Ottawa, ON K1A 0G1, Canada

<sup>2</sup>Department of Mechanical and Mechatronics Engineering, University of Waterloo, Waterloo, ON N2L 3G1, Canada

\*Corresponding author, email rashidasy@yahoo.ca



a original interface; b fracture of brittle oxide layer; c first requirement: aligned oxide layer cracking; d second requirement: metal to extrude through cracks

### 1 Schematic of oxide layer cracking and formation of metal-to-metal contact<sup>17</sup>

worksheet (E/W) interface is also important and can affect the nugget size and electrode degradation behaviour.<sup>6-8</sup> Important characteristics of the aluminium worksheet surface which influence the electrical contact resistance and hence the RSW process are the presence of an oxide layer, roughness of the surface, and presence of a chemical or lubricant. While roughness could alter this electrical contact resistance,<sup>9,10</sup> the oxide layer is considered to be the main reason for high contact resistance at the interface.<sup>4,11</sup> The presence of a chemical or lubricant is also considered to be influential on the electrical contact resistance.<sup>11,12</sup>

An oxide layer at the surface of aluminium is always present and quickly reforms if removed mechanically or by a chemical action. This oxide layer on the aluminium (worksheet) surface may not be uniform and other oxides and hydroxides could also be present.<sup>11,13</sup> In addition, this layer is very hard and has very high electrical resistance,<sup>14</sup> which makes it difficult to penetrate for electrical conductivity. Cracking and/or removal of the oxide layer is essential for successful spot welding as the current flow through the interfaces is only possible through a few contact points where this layer is cracked and establishes a metal-to-metal contact.<sup>4,11</sup> Surface roughness makes it more complex because the actual contact area which bears the load when two surfaces pressed against each other is much smaller than the nominal contact area.<sup>15</sup> Studer<sup>16</sup> suggested that, for aluminium alloys, even in the actual contact area there were only few points where a metal-to-metal contact was established. Straining the surface layer was found to be effective in cracking the surface oxide layer of aluminium which cracked in a brittle manner due to straining of sheet surface.<sup>17</sup> The study<sup>17</sup> also endorsed Studer's<sup>16</sup> idea that the metal-to-metal contact was only established when the cracks on both the surfaces aligned and base metal extruded through them (Fig. 1).

The location where melting starts at the FS during RSW process is also very important and could influence

the nugget properties and the RSW process.<sup>6,18-20</sup> Since the metal-to-metal contact is established at only a few points in the entire contact area of the FS, predicting these locations for a particular spot weld is quite challenging. Particularly, this knowledge is not well established when using spherical tip electrodes for RSW of aluminium alloys. Tsai *et al.*,<sup>18</sup> through finite element analysis (FEA), suggested that the melting at the FS started in a ring around the centre when using a flat tip electrode for steel. However, no experimental evidence for this ring melting was presented. Applying a high current for a short time could cause peripheral melting at the FS as suggested for both steel<sup>19</sup> and aluminium.<sup>20</sup> For aluminium alloys, Thornton *et al.*<sup>20</sup> found local melting around the centre due to well established contact between the surfaces at the periphery of the FS interface. They used flat tip electrodes and considered that behaviour as an extreme case of a failed spot weld. However, the knowledge of oxide layer behaviour at the FS and the resulted nugget formation is still not well established for RSW of aluminium alloys.

Another phenomenon that can also disturb the surface morphology is the sheet separation that occurs during the squeezing phase of the RSW process. Worksheet separation occurs from the end of the contact which defines the contact area at the FS. This contact area grows gradually outward during the squeezing hence shifting the separation point away from the centre.<sup>21</sup> Electrode geometry is influential on this separation and spherical electrodes produce less sheet separation than flat tip electrodes.<sup>22</sup> Although, sheet separation appears to be an important characteristic of RSW of aluminium alloys, the authors are not aware of any detailed tribological and/or metallurgical research effort which relates this phenomenon to the nugget formation and growth.

The purpose of the present work is to investigate the contact behaviour at the FS interface. The main

objective is to understand the oxide layer behaviour during the squeezing phase of the RSW process and related nugget growth pattern during the current phase of the RSW process of aluminium alloys. Series of experiments were conducted to observe the start of melting at the FS and the nugget formation and growth behaviour. Finite element analysis was conducted for the squeezing phase of the RSW process. Experimental observations and FEA were analysed in details to explain the FS interaction and resulting nugget formation process.

## Materials and methods

Aluminium alloy 5182 sheets (AA5182) containing 4.71%Mg as a major alloying element were used as worksheet materials for the entire study. The nominal thickness of the worksheets was 1.5 mm with a chemical composition of 4.71Mg–0.32Mn–0.19Fe–0.08Si–0.05Cu–0.01Zn (wt-%). The entire study was performed on the as received worksheet surface without any chemical or mechanical treatment. The centerline average surface roughness  $R_a$  of the worksheet was measured as  $0.32 \pm 0.02 \mu\text{m}$ . While characterising the worksheet surface, it was observed that the general surface morphology was not uniform over the entire surface. In another work<sup>23</sup> on similar material with similar welding condition, it was observed that there were several spots on the worksheet surface that had higher contents of Mg and O than the general surface area. Those spots were suggested to be magnesia or MgO. It is therefore believed that the worksheet surface of AA5182 had non uniform oxide layer with the presence of MgO along with alumina ( $\text{Al}_2\text{O}_3$ ). Although a direct measurement of this oxide layer thickness was not performed in this study, in line with other studies,<sup>10,13</sup> the oxide layer thickness was expected to be in the range of 7–12 nm.

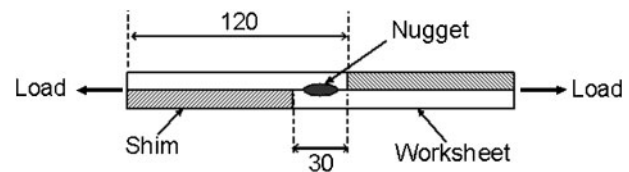
The RSW process was performed using class I type<sup>24</sup> spherical tip copper electrodes with face diameter 10 mm and radius of curvature 50 mm. A 170 kVA pedestal type medium frequency direct current spot welder was used for the RSW process. More details about these materials, geometry and welding equipment were provided in another work.<sup>7</sup> Unless otherwise mentioned, all RSW was performed using parameters (Table 1) that had been selected based on a series of preliminary investigations of RSW with this alloy.

### Nugget formation, growth and shape experiments

The purpose of these experiments was to observe the nugget formation and growth pattern. Resistance spot welding was performed with different current times (1–5

**Table 1** Welding parameters and weld schedule (1 cycle=16.67 ms)

Force	6 kN
Current magnitude	29 kA
Weld rate	20 spots/min
Squeeze time	25 cycles
Current time	5 cycles
Hold time	12 cycles



**2** Geometry of overlapped shear test specimen with shims

cycles where 1 cycle=16.67 ms) on overlapped specimens of 30 × 120 mm with an overlap of 30 mm (Fig. 2). Other than current time, all other welding parameters were kept constant at the values given in Table 1 and this included squeezing for 25 cycles (before the current was applied) plus holding for 12 cycles after the current had been applied. Three sets of experiments were performed each with a fresh pair of electrodes. Typical nugget cross-sections for all these welds were performed using a standard metallographic procedure up to the stage of manual grinding with 1200 silicon carbide papers and further polishing was not considered necessary to view the nuggets. However, a typical set of these nugget cross-sections were prepared completely up to the last stage of polishing and viewed through optical microscope to obtain a very precise view.

Experiments of RSW were also conducted to monitor the joint shear force at different current times. Five samples were used for each current time and the welding process was randomised to avoid any sequential effect (Table 2). Similar procedure, as described above, was employed and welded samples were subjected to tensile testing. Some overlapped samples were also subjected to spot welding using both the low current time and low current magnitudes; the intent of such experiments was to monitor the shape of the nugget at low currents.

### Start and progress of melting experiments

Initially, several spot welds were performed using 10 and 15 kA on overlapped samples for different current times. Local melting at some locations of the FS interface was observed in these spot welds. A complete set of RSW was then performed on similar overlapped samples using currents in the range of 10–20 kA with an increase of 1 kA; for each current magnitude, the current was applied for only 1 cycle. Resistance spot welding was also performed on overlapped samples using current magnitudes of 10 and 15 kA for different current times (1–5 cycles) for each current (Table 3).

### Testing and metallography

Shear tests of spot welded overlapped samples were performed using Instron tensile testing machine (model-4206; Instron, Canton, MA, USA). Shims were used (Fig. 2) to minimise any twisting of the samples during these tests.<sup>20</sup> Standard metallographic procedure was adopted and polished samples were etched with Keller's reagent for ~15 s and then rinsed with warm water.<sup>25</sup> All surfaces were analysed using standard optical and stereo microscopes. For higher resolution images, scanning electron microscopy (SEM) was performed using Jeol JSM 6460 microscope (Jeol Ltd, Tokyo, Japan).

## Finite element analysis

For sheet separation and other contact behaviour at the FS during the squeezing phase of the RSW process, FEA was conducted using a commercial code (ABAQUS Hibbit, Karlsson & Sorensen Inc., Pawtucket, RI, USA).<sup>26</sup> An axisymmetric elastic-plastic model was developed to simulate the actual welding process for the squeezing phase of the RSW process. The model consisted of both upper and lower electrodes with both worksheets. The model simulated the experimental forces and boundary constraints by allowing upper electrodes to move down while keeping the lower electrode fixed in the axial direction. A loading function similar to that of actual load behaviour during the squeezing force was used for the model. Details of the formulation of the model could be found in a previous work.<sup>7</sup> Although, symmetry exists at the FS and no shear stress was expected, an appropriate coefficient of friction of 0.8 was used for this interface.<sup>27</sup>

## Results

### Nugget formation, growth and shape

A typical set of nugget cross-sections for various current times showed several interesting features (Fig. 3). Although smaller, the nugget seemed to be completely formed after applying the current for 1 cycle. In general, aluminium alloys need high currents for short current times. When selecting the welding parameters for the present material, it was observed that 1 current cycle (16.67 ms) at 29 kA was not long enough to get the proper joint properties. However, the apparent formation of a complete nugget during the first current cycle showed difficulties associated with monitoring the real

nugget growth pattern for this material. Since 1 cycle was the minimum time that the spot welding machine could apply, it was considered possible that even less than 1 cycle might be sufficient to allow nugget formation at this current level.

It can be seen that each of these weld nuggets has some voids (porosity) at the center of the nugget. Porosity in resistance spot weld nuggets is very common and is more common in aluminium alloys than steel. These voids result from the gaseous bubbles trapped in the liquid pool and volume shrinkage during the cooling phase of nugget formation.<sup>28</sup> The gaseous bubbles in the weld nugget result from the volatile alloying elements such as Mg and Zn. At the centre of the molten pool where the temperature is highest, these elements may evaporate to form the gaseous bubbles. As the solidification begins after the current is seized, these gaseous bubbles are trapped between the solids to create voids which are generally revealed by cross-section metallography of the spot welded nuggets. On the other hand, the shrinkage of the nugget pool during the cooling process can also produce microvoids. Although, these voids are much smaller than gaseous bubbles, they can combine together and/or with the gaseous bubbles to form large voids in the nugget pool. Since Mg is the major alloying element of AA5182, the voids observed in Fig. 3 are very common and studies on similar material have also shown these voids.<sup>12,29</sup>

An interesting observation from these experiments was the nugget growth with current time. The nugget size grew with current time and a faster growth rate was observed for the first current cycle after which the nugget expansion occurred gradually. This finding was supported by the joint shear force values measured for

**Table 2 Test matrix of RSW process involving different current times (1 cycle=16.67 ms)**

Electrode pair	Current magnitude, kA	Current time, cycles	Test sequence
I	29	3	1st
		1	2nd
		2	3rd
		4	4th
		5	5th
II	29	2	1st
		4	2nd
		3	3rd
		5	4th
		1	5th
III	29	4	1st
		3	2nd
		5	3rd
		1	4th
		2	5th
IV	29	1	1st
		4	2nd
		2	3rd
		5	4th
		3	5th
V	29	5	1st
		2	2nd
		1	3rd
		3	4th
		4	5th

the RSW process (Table 2) and plotted against the current time (Fig. 4). Two visible growth rates (slopes) were observed; the growth rate during the first current cycle was much higher than the growth rate during the last 4 cycles. This observation was in line with other studies<sup>20,30</sup> which reported that the electrical contact resistance of the FS, during RSW of aluminium alloys, dropped sharply during the first current cycle and remained very low during the remaining current time. Obviously, a high resistance in the beginning would cause more heat generation than during the remaining current time which was the case here.

Another interesting observation from Fig. 3 was the shape of the nugget itself. These nuggets were not exactly elliptical; rather they were elliptical from the two ends but had less height at the centre. This shape of the nugget gave the indication that two ellipses grew and merged with each other and produced a nugget which had a shape that resembled a doughnut but without a hollow middle section. This shape of the nugget was very obvious in the beginning (after the first and second current cycles) of the nugget formation but still remained visible at the end of the 5 cycles. Figure 5 shows another typical example of this shape of the nugget when RSW of AA5182 was carried out for a lower current of 20 kA for a current time of 1 cycle. The shape of these nuggets suggested that the melting at the FS did not start in the centre; rather it started at an intermediate radial distance from the centre and grew both inwards and outwards. The growth was more extensive in the inward direction and merged to form a continuous nugget. This general doughnut shaped nugget was observed for all cases, particularly at shorter current times, although there were few minor differences in porosity.

### Start and progress of melting

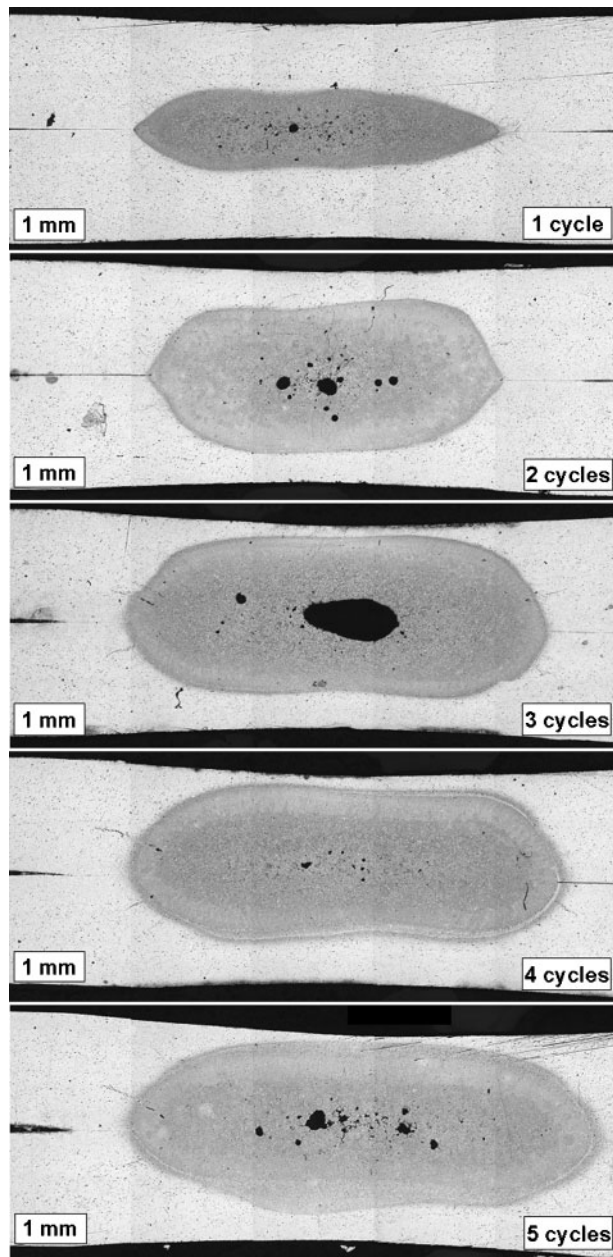
Since complete nugget formation was observed for low currents and short current times (Figs. 3 and 5), it was

quite difficult to locate the start of melting at the FS and thus, RSW of AA5182 sheets was performed for very low currents (10–20 kA) not appropriate for successful RSW of AA5182. Figure 6 shows typical SEM micrographs of the melting process at the FS while performing RSW for low currents and short current times (test sequence 1–11, Table 3). It can be observed that the melting occurred at various spots in the contact zone of the FS. The size and number of these spots increased with increasing current magnitude. It was observed that all of those melted spots were located near the periphery of the contact without any significant melting at the centre of the FS interface. For higher currents (15–20 kA) within this range, these spots grew and merged to form a very clear melted ring around the centre. Interestingly, the locations of these melted spots (outer diameter) were in the range of 4.0–5.0 mm. It is important to note that because of the variability of these experiments, it is possible that for some high currents (e.g. 20 kA), melting could reach the centre while performing RSW for the same current time of 1 cycle as shown in Fig. 5.

This melting behaviour suggested that at the beginning of the nugget formation, there was more heat generation at the periphery than at the centre. Even at 20 kA, there was melting in the ring near the periphery while the central portion was still not yet melted completely. Chang *et al.*<sup>29</sup> performed FEA for similar welding conditions and compared it with experiments. Although, their FEA showed an elliptical nugget, the experimental nugget appeared similar to those presented earlier in Fig. 3. They reported high current density at the periphery during the initial stage of the weld phase but did not mention this shape in their work. Kaiser *et al.*<sup>19</sup> reported that high current and short current time caused peripheral melting when using flat tip electrode for steel. They believed that the peripheral zone at the FS provided good metallic contact and hence was the

**Table 3 Test sequence of RSW involving different current magnitudes and current times (1 cycle=16.67 ms)**

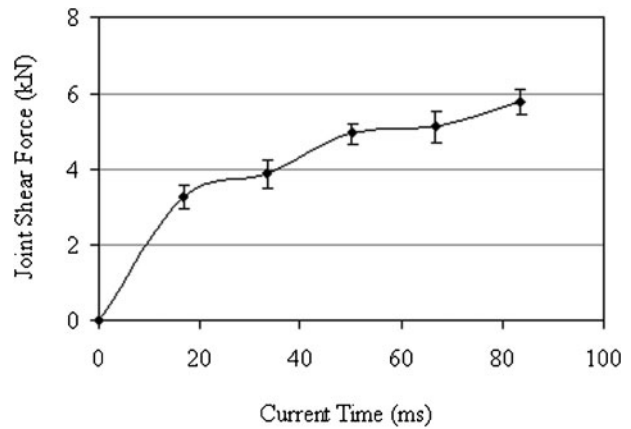
Electrode pair	Current magnitude, kA	Current time, cycles	Test sequence
VI	10	1	1st
	11	1	2nd
	12	1	3rd
	13	1	4th
	14	1	5th
	15	1	6th
	16	1	7th
	17	1	8th
	18	1	9th
	19	1	10th
	20	1	11th
	10	1	12th
	10	2	13th
	10	3	14th
	10	4	15th
	10	5	16th
	15	1	17th
	15	2	18th
	15	3	19th
	15	4	20th
	15	5	21st



3 Nugget cross-sections showing shape and nugget growth with increasing weld time (1–5 cycles)

least resistance zone because it deformed easily. Although, these works showed peripheral melting, none of the work showed a doughnut shaped nugget as presented here. Also, not much detail was provided about the surface interaction that actually happened at the FS during squeezing process particularly for the RSW of aluminium alloys.

Welding for different current times (1–5 cycles) at low currents of 10 and 15 kA showed the melting growth pattern at the FS. Similar behaviour was observed for both current magnitudes and a very clear observation of melting growth at 10 kA (test sequence 12–14, Table 3) is presented here (Fig. 7). Once again it was observed that the melting started at the periphery and proceeded inwards with increasing weld time. It was observed that



4 Average joint shear force of RSW when welded for different weld times

the central portion of the FS was heat affected at the end of 3 cycles; however, there was no melting of the sheet metal even at the end of 3 cycles.

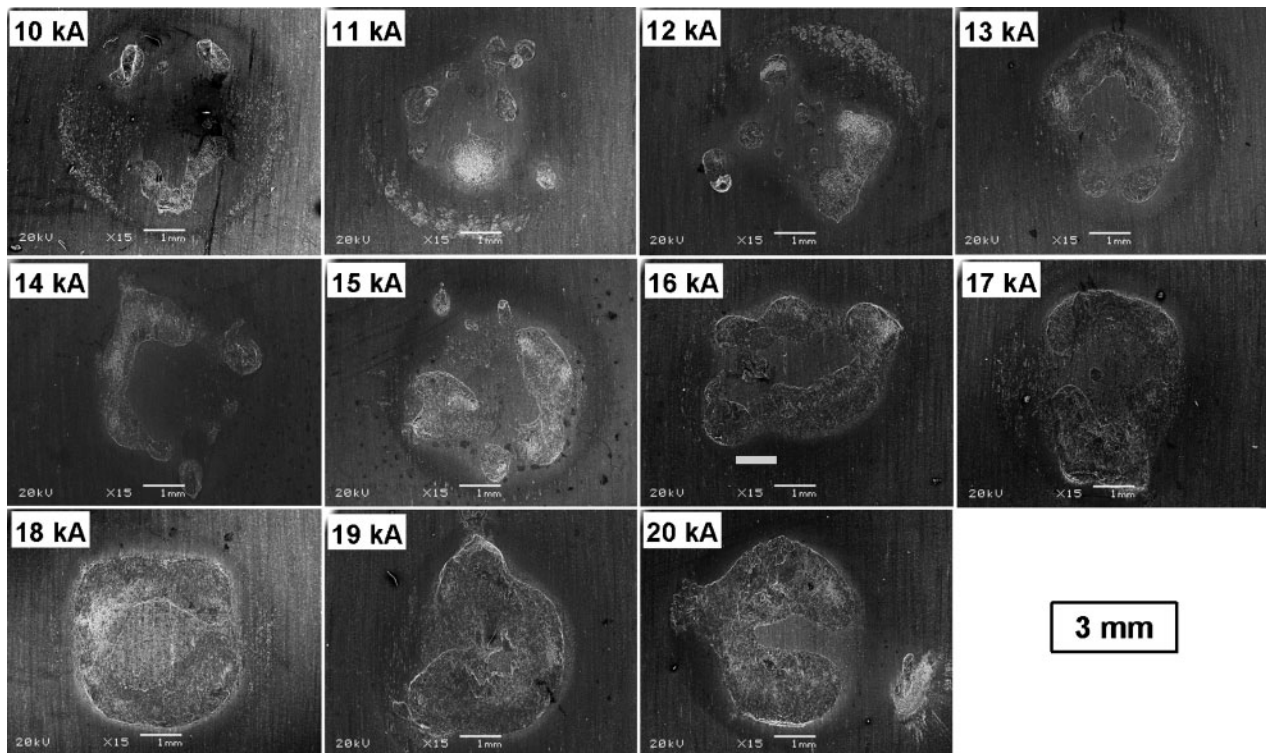
It is important to mention here that the spontaneous melting observed above would appear as several small nuggets in the cross-section view of these nuggets. However, these spots would be too shallow and too small to be considered a proper spot weld nugget<sup>28</sup> because a proper spot weld nugget should have a diameter equivalent to four times the square root of the worksheet thickness ( $4t^{1/2}$ ).<sup>24</sup> For the present worksheet material ( $t=1.5$  mm), this nugget diameter should be 4.9 mm or bigger to be a proper weld nugget. Therefore, a weld nugget with several such small melted spots that resulted from insufficient current and/or current time would be considered as a failed nugget.

### Discussion

The results presented above clearly showed that during the RSW of AA5182, melting at the FS started in a ring near the periphery and grew inwards from all sides and merged to form a complete nugget with central contact zone melts at the end of nugget formation. Experimental observations were analysed along with FEA results to explain the different steps of nugget formation during RSW of AA5182.



5 Shape of nugget after RSW of AA5182 with 20 kA for 1 current cycle



6 Images (SEM) showing heat generation and start of melting at FS spot welded at low currents (10–20 kA) for weld time of 1 cycle

### Contact pressure and contact diameter

Contact pressure distribution at the FS interface showed the highest value at the centre and dropped to zero at the end of the contact (Fig. 8). This pressure distribution was typical for RSW of aluminium alloys with spherical electrodes and similar FEA results were reported earlier<sup>31</sup> for aluminium alloys. The pressure distribution was also used to define the contact diameter at this interface which was found to be 5.4 mm and showed good agreement with the experimental values ( $5.3 \pm 0.04$  mm). Five overlapped specimens were used and the contact diameter at the FS after squeezing was measured by placing carbon imprints between the worksheets during squeezing. It was observed both experimentally and analytically (FEA) that the contact diameter of the FS was just a little larger than that of the

E/W interface (Fig. 9). Other FEA analyses<sup>29,31</sup> showed similar behaviour where the contact diameter of the FS was reported a little higher than that of the E/W interface.

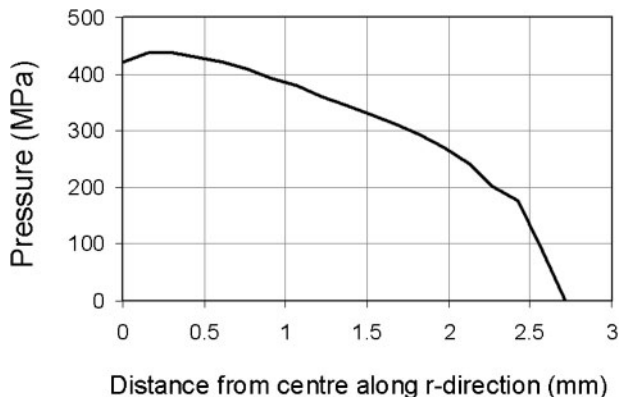
### Sheet separation

The most significant of the FEA results was the sheet separation from the end of the contact at the FS (Fig. 10). Sheet separation is a typical characteristic that occurs during RSW, particularly during RSW of aluminium alloys.<sup>22</sup> Sheet separation due to squeezing was also observed through experiments. Strips of AA5182 sheet of size  $120 \times 30$  mm were used for these experiments. Two such strips were brought in complete overlap with each other to make a sample. These samples were squeezed between electrodes with the same force of 6.0 kN as that used for actual welding and sheet



a 1 cycle; b 2 cycles; c 3 cycles

7 Start and progress of heat generation (melting) at FS spot welded at low current of 10 kA for different weld times

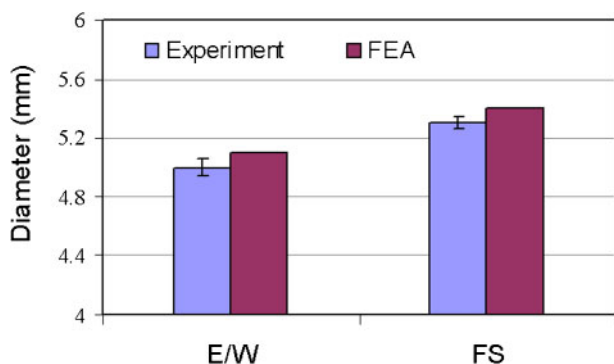


8 Distribution of contact pressure at FS during squeezing

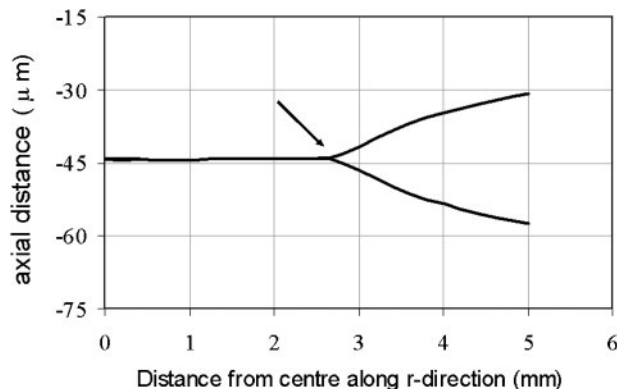
separation was measured at a distance of 60 mm from the centre (Fig. 11). Ten measurements were obtained and the average sheet separation (A in Fig. 11) was found to be  $91 \pm 13 \mu\text{m}$ . The space available around the electrode in the spot welder did not allow measuring the sheet separation accurately anywhere closer to this, 60 mm from the centre and therefore, an exact comparison of the experimental values with that of FEA results was not possible and not discussed here. Importantly, the sheet separation was observed both experimentally and from FEA.

### Effect of sheet separation

As mentioned earlier, oxide layer on aluminium sheet surface was very hard compared with the base metal and fractured in a brittle manner under straining.<sup>17</sup> Sheet separation, from the end of the contact, acted like bending and although, an oxide layer was not included in FEA, in reality, the bending of sheet from the end of the contact could cause the fracture of the hard oxide layer. To evaluate the effect of bending due to sheet separation on the worksheet surface layer, exaggerated bending was produced to enhance the effect of bending. Samples similar to those used in sheet separation measurements were clamped from the centre and force was applied to produce exaggerated bend in the sheets. Plain and bent surfaces, taken from the same samples, were observed through SEM and typical micrographs are presented (Fig. 12). Two significant effects on the



9 Contact diameters of FS and E/W interface obtained experimentally and through FEA



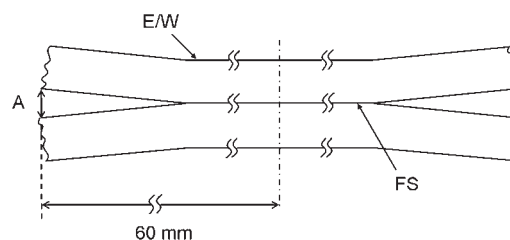
10 Axial position of FS after squeezing showing sheet separation from end of contact at this interface

bent surfaces were observed: the cracks on the bent surface got enlarged due to bending; and these cracks got aligned at several locations to produce larger cracks. These sorts of large and aligned cracks were not observed on the plain sheet surface (Fig. 12a).

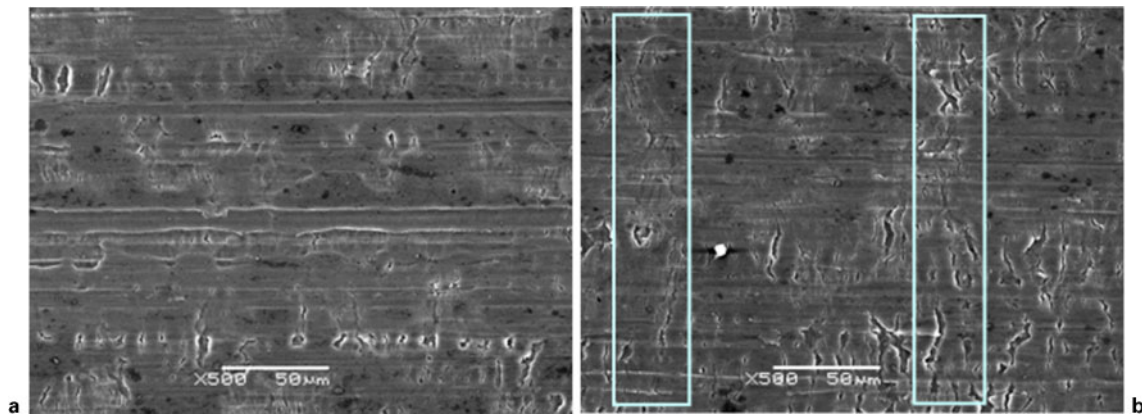
The actual sheet separation during the squeezing had much less bending than the exaggerated bending as shown above and hence the effect of squeezing on the surface layer cracking was not expected to be as obvious (macro) as shown in Fig. 12. However, owing to the hardness of the oxide layer, a similar effect with less intensity was expected. With the help of high resolution SEM at higher magnifications, it was possible to locate such effect, to a lesser extent, on some squeezed samples. The FS of all of the specimens used for sheet separation measurements were observed through SEM and two obvious effects of sheet separation on the surface layer cracking are presented (Fig. 13). Once again, some significant and aligned cracks were observed along the periphery; importantly, these kinds of aligned cracks were not visible anywhere else in the entire contact zone.

### Location of sheet separation

The FEA results also showed that the location of sheet separation during squeezing was moving with the increasing load. It was observed that the sheets were separated as early as the loading started and the location of sheet separation as well as the amount of sheet separation changed with increasing loads. The initial location, where an obvious sheet separation occurred during the early stage of loading, was observed at a diameter of 4.0 mm. With increasing load, this location moved away from the centre and at full load of 6 kN



11 Sheet separation due to squeezing: average value of A is  $91 \pm 13 \mu\text{m}$



a plain sheet surface; b bent sheet surface

**12 Effect of sheet separation on oxide layer cracking: enlarged and aligned cracks are visible on bent surface**

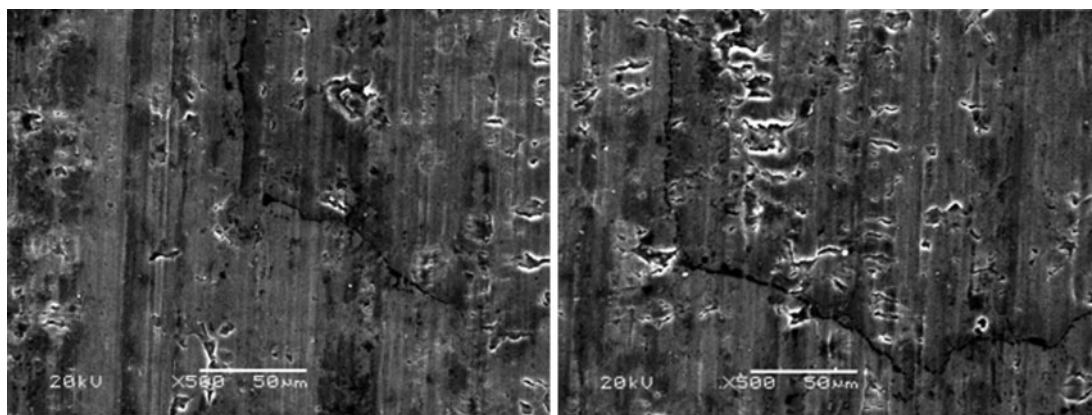
after 5 cycles (0.083 s), sheet separation was located at the end of the contact at this interface (Fig. 14). The effect of sheet separation on the surface (oxide) layer cracking was already explained earlier in this section. The movement of the location of sheet separation with load indicated that the oxide layer cracking during squeezing started very early. However, with increasing load, contact area at the FS grew and collapsed sheets near the periphery. Interesting to note here that although, the contact pressure dropped to zero at the end of the contact, it remained significant in the range of 4.0–5.0 mm (Fig. 8). These observations clearly suggested that near the periphery of the contact at the FS there would be more cracks in the oxide layer and the contact area in this zone would have some significant amount of metal-to-metal contacts.

**Nugget formation model**

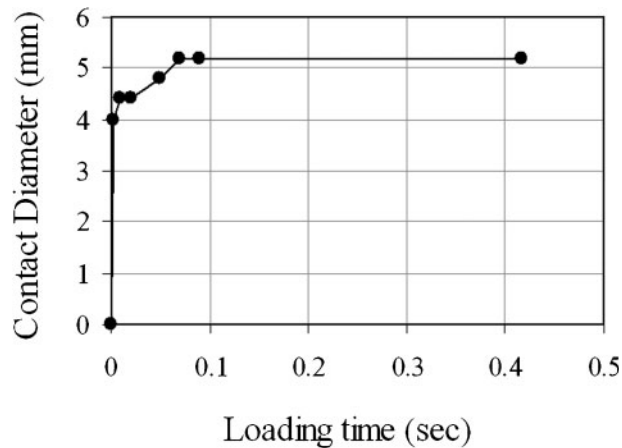
Through experimental observations and FEA results, the contact behaviour at the FS can be explained to understand the ‘nugget formation’ during RSW of AA5182. It was already mentioned that the current flow through this interface was only possible through metal-to-metal contacts. In the entire contact zone, there could be several cracks at each surface. However, at the periphery of this interface, due to sheet separation, there would be exaggerated cracks in the surface oxide layer of

both the worksheets. The chances that the cracks from both the sheets would align with each other would be much higher near the periphery and hence the chances of metal-to-metal contacts would be higher as well. On the other hand, in the central contact zone, there could be several cracks on each surface. However, there would be only few spots<sup>16,17</sup> where those cracks would have aligned to produce metal-to-metal contacts. The more the area of the metal-to-metal contact, the less would be the constriction resistance. At the start of the weld current, the periphery of the contact at the FS would provide the preferred (least resistance) flow path for the current through this interface. This would cause current concentration and high heat generation at the periphery of the FS hence the start of melting would occur near the periphery (Fig. 15). With increasing current time, the melting would proceed in all directions and merge to produce a complete nugget of doughnut shape.

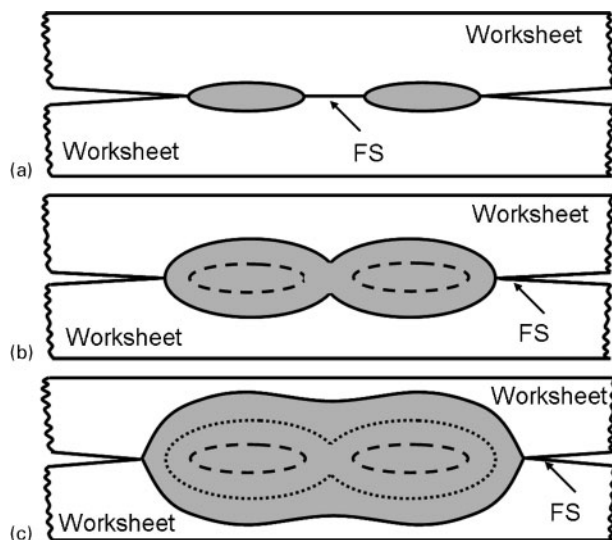
In the context of the nugget formation model discussed above, it is important to mention that the overall all constriction resistance at the FS will be decreased with the increasing number of metal-to-metal contacts within the contact zone of this interface. As mentioned above, current prefers to flow through low resistance path. Therefore, if the number of metal-to-metal contact spots in the central contact zone of the FS is increased, the melting could also start from the centre



**13 Visible cracks on worksheet surface observed near periphery of contact at FS**



14 Location and movement of sheet separation at different stages of squeezing



a start of heating at periphery; b heating growth more rapidly inwards than outwards; c completion of weld nugget

15 Start of melting and nugget growth model for RSW of AA5182

and the nugget would get a different shape. However, due to the process mechanics of RSW of aluminium alloys, the periphery of the contact at the FS was found to be the preferred area where most metal-to-metal contacts would develop and result in the shape of the nugget as proposed here.

## Conclusions

Surface interaction at the FS interface during the RSW of AA5182 was studied experimentally and with FEA. Factors influencing the melting and nugget formation were identified and investigated. The major findings are summarised as follows.

1. The contact behaviour at the FS during squeezing process was found to be very important for the

outcome of RSW process. The tribological interactions at the FS during squeezing had significant effect on the start of melting and hence the nugget formation.

2. A complete weld nugget was formed at the end of the first current cycle and grew larger during the remaining current time. The heat generation at this interface was higher during the first current cycle than the remaining weld time and this was confirmed by joint shear force measurements and the rate of nugget growth.
3. Experimental observations as well as FEA indicated sheet separation and thus sheet bending at the end of the contact zone of the FS. The sheet separation was significant near the periphery and is expected to produce high surface strains that could have disrupted the oxide layer on the worksheet surface.
4. The melting at the FS did not start at the centre of the contact; rather it started at the periphery at a diameter between 4.0 and 5.0 mm. This melting around the periphery proceeded rapidly towards centre to form a complete weld nugget. This pattern of melting produced nuggets which resembled a 'doughnut' with a thin central plug filling the hole.

## Acknowledgements

This study was supported by the Natural Science and Engineering Research Council (NSERC) and the Automobile of the 21st Century (Auto21), one of the Networks of Center of Excellence (NCE) programs, both established by the Canadian Government.

## References

1. B. Irving: *Weld. J.*, 1995, 74, (8), 29–34.
2. R. Ikeda, K. Yasuda and K. Hashiguchi: *Weld. World*, 1998, 41, 492–498.
3. C. J. Newton: Proc. Sheet Metal Welding Conf. IV, Detroit, MI, USA, October 1994, AWS, Paper E2.
4. P. S. James, H. W. Chandler, J. T. Evans, J. Wen, D. J. Browne and C. J. Newton: *Mater. Sci. Eng. A*, 1997, A230, 194–201.
5. A. De: *Sci. Technol. Weld. Join.*, 2002, 7, (2), 119–124.
6. J. A. Khan, L. Xu and Y. J. Chao: *Sci. Technol. Weld. Join.*, 1999, 4, (4), 201–207.
7. M. Rashid, J. B. Medley and Y. Zhou: *Sci. Technol. Weld. Join.*, 2009, 14, (4), 295–304.
8. I. Lum, S. Fukumoto, E. Biro, D. R. Boomer and Y. Zhou: *Metall. Mater. Trans. A*, 2004, 35A, 217–225.
9. P. H. Thornton, A. R. Krause and R. G. Davies: *Weld. J. Res. Suppl.* 1997, 76, (8), 331s–341s.
10. E. Crinon and J. T. Evans: *Mater. Sci. Eng. A*, 1998, A242, 121–128.
11. E. P. Patrick, J. R. Auhl and T. S. Sun: 'Understanding the process mechanism is key to reliable resistance spot welding aluminum autobody components', SAE technical paper no. 840291, SAE, Warrendale, PA, USA, 1984, 1–14.
12. M. Rashid, S. Fukumoto, J. B. Medley, J. Villafuerte and Y. Zhou: *Weld. J. Res. Suppl.*, 2007, 86, (3), 62s–70s.
13. J. C. Kucza, J. R. Butruille and E. Hank: 'Aluminum as-rolled sheet for application-effect of surface oxide on resistance spot welding and adhesive bonding behavior', SAE technical paper no. 970013, SAE, Warrendale, PA, USA, 1997, 11–22.
14. in 'Engineering materials handbook', Vol. 4, 'Ceramic and glasses'; 1991, Materials Park, OH, ASM International.
15. J. A. William: 'Engineering tribology'; 1994, Oxford, Oxford University Press

16. F. J. Studer: *Weld. J. Res. Suppl.*, 1939, 18, 374s–380s.
17. H. A. Mohamed and J. Washburn: *Weld. J. Res. Suppl.*, 1975, 54, (9), 302s–310s.
18. C. L. Tsai, O. A. Jamal, J. C. Papritan and D. W. Dickinson: *Weld. J. Res. Suppl.*, 1992, 71, 47s–54s.
19. J. G. Kaiser, G. J. Dunn and T. W. Eager: *Weld. J. Res. Suppl.*, 1982, 61, 167s–174s.
20. P. H. Thornton, A. R. Kruse and R. G. Davies: *Weld. J. Res. Suppl.*, 1996, 75, 402s–412s.
21. H. Zhang, Y. J. Huang and S. Jack Hu: Proc. Sheet Metal Welding Conf. VII, Detroit, MI, USA, October 1996, AWS, Paper B3.
22. R. Ikeda, K. Yasuda, K. Hashiguchi, T. Okita and T. Yahaba: Proc. IBEC'95 on 'Advanced technologies and processes', Detroit, MI, USA, October 1995, SAE, 144–151.
23. M. Rashid: *J. Mater. Eng. Perform.*, 2010, DOI: 10.1007/s11665–010–9696-z.
24. D. Giroux and F. D. James: 'Resistance welding manual', 4th edn; 2003, Philadelphia, PA, RWMA.
25. in 'ASM handbook', Vol. 9, 'Metallography and Microstructure'; 1985, Metals Park, OH, ASM International.
26. ABAQUS user's manual-interactive version 6.5, 2004. Hibbit, Karlsson & Sorensen Inc., Pawtucket, RI, USA
27. in 'Metals handbook', 10th edn, Vol. 18, 'Friction, lubrication, and wear technology'; 1990, Materials Park, OH, ASM International.
28. H. Zhang and J. Senkara: 'Resistance welding: fundamentals and applications'; 2006, Boca Raton, FL, Taylor and Francis Group.
29. B. H. Chang, Y. Zhou, I. Lum and D. Du: *Sci. Technol. Weld. Join.*, 2005, 10, (1), 61–66.
30. M. Hao, K. A. Osman, D. R. Boomer and C. J. Newton: *Weld. J. Res. Suppl.*, 1996, 75, (1), 1s–8s.
31. X. Sun and P. Dong: *Weld. J. Res. Suppl.*, 2000, 79, (8), 215s–221s.